LEHIGH UNIVERSITY
DEPARTMENT OF CIVIL ENGINEERING AND MECHANICS
BETHLEHEM, PA.

ADDRESS REPLY TO:
FRITZ ENGINEERING LABORATORY

PHONE
BETHLEHEM 7-5071
FRITZ E. L. OFFICE EXT. 258
HYDRAULICS LAB. EXT. 279

File : 205A

ERRATA:

to Robert L. Ketter and Lynn S. Beedle, "The Moment-Curvature Relation for WF Columns", Progress Report P, Fritz Laboratory Report No. 205A.10, September 1952.

page 2 Fig. 1(b) the equation should read

$$M = \int_A y \sigma \, dA$$

page 5 Equation (3) should read

$$M = \int_A y \sigma \, dA$$

page 14 Equation (5M) should read

$$M = (\sigma_y - \sigma_a)\left[\frac{w}{12 y_c}(y_c - t)^2(3d - 2y_c - 4t) + \frac{bt}{12 y_c}(6y_c d - 6y_c t - 3dt + 4t^2)\right]$$

WELDED CONTINUOUS FRAMES & THEIR COMPONENTS

PROGRESS REPORT P

THE MOMENT - CURVATURE RELATION FOR WF COLUMNS

(Not for Publication)

by

Robert L. Ketter & Lynn S. Beedle

This work has been carried out as part of an investigation sponsored jointly by the Welding Research Council, and the Navy Department with funds furnished by the following:

American Institute of Steel Construction
American Iron and Steel Institute
Column Research Council (Advisory)
Institute of Research, Lehigh University
Office of Naval Research (Contract No. 39303)
Bureau of Ships
Bureau of Yards and Docks

Fritz Engineering Laboratory
Department of Civil Engineering and Mechanics
Lehigh University
Bethlehem, Pennsylvania

September, 1952

Fritz Laboratory Report No. 205A.10

TABLE OF CONTENTS

I INTRODUCTION

When extending the methods of analysis used in engineering mechanics to include the case of elastic-plastic bending, the relation between applied moments, axial thrust and resulting curvature for the case where stresses exceed the elastic limit is basic in importance, since it is the integrated effect of this curvature that determines deflections and rotations. The value of moment-deflection data is primarily that it allows the determination of true maximum loads. Moment-rotation data is also valuable since it enables one to evaluate performance relating to energy absorption.

One assumption that must be made is that the Bernoulli-Navier hypothesis (bending strain is proportional to the distance from the neutral axis) can be extended to include the case of plastic deformations.* Using this together with assumptions with regard to properties of the material in question, this report will outline and illustrate a method whereby a relation between axial loads, bending moment and curvature can be obtained even though stresses exceed the elastic limit.

The curvature, ϕ, is a function of the strain developed at a section; the moment, M, is a function of the resultant stress. These ideas are illustrated in Fig. 1(a) and 1(b).**

---

* Actually for steel members this is an idealization. As has been described in previous work[1], it is only required that in the elastic range, the strain be proportional to the distance from the neutral axis and in the plastic range the stress be equal to the lower yield-point stress. Thus the curvature at any section is a function of the part which remains elastic. This is further discussed in section II of this report.

If the strain-hardening range is considered, it is once again necessary to make an assumption with regard to strain-distribution in the inelastic range. But strain-hardening has not been considered in this paper.

** Details of the development of these equations are given on page 46 of Reference (2).

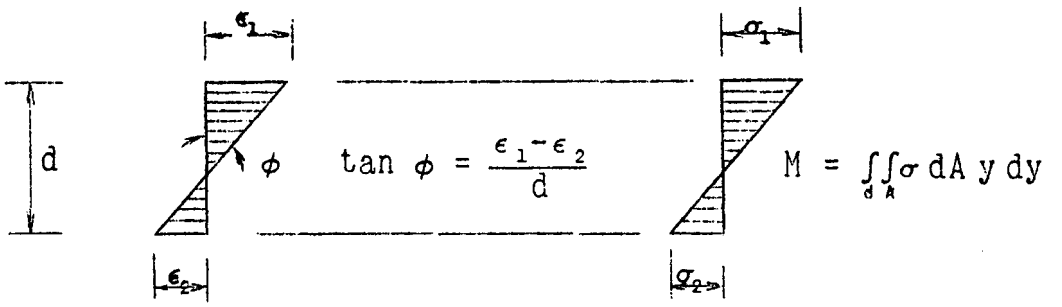

Fig. 1

For the case of elastic strains illustrated in Fig. 1 (that is, when $\epsilon_1 < \epsilon_y$ and $\epsilon_2 < \epsilon_y$) the distribution of strain and distribution of stress are similar, σ_1 being equal to $E\epsilon_1$, etc. When yielding occurs, however, this linear relation no longer holds. Instead there results a stress distribution composed of segments of various straight lines or curves depending on the stress-strain properties of the material in question.

For this report in agreement with those preceeding it, the idealized stress-strain diagram of Fig. 2 has been assumed. This curve closely approximates the experimental stress-strain diagram of mild structural steel in the elastic and plastic ranges. Strain hardening is neglected.

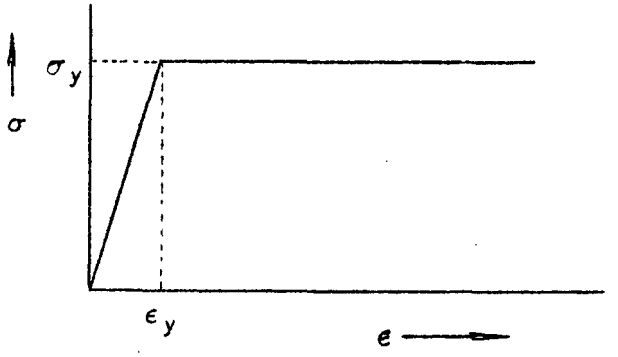

Fig. 2

The effect of this choice on the stress and strain distribution curves, when strains exceed the elastic limit, is shown in Fig. 3.

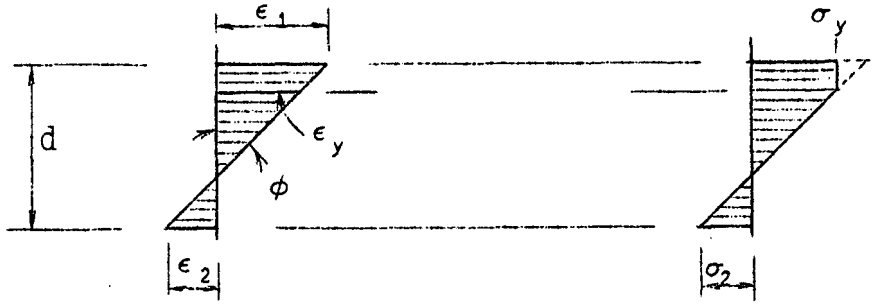

Strain Diagram (a) Stress Diagram (b)

Fig. 3

As would be expected, the moment corresponding to a given value of ϕ would be less than that predicted using the straight line relation of the elastic solution.

The problem of determining M-ϕ relations in the plastic range has been solved for the condition of pure bending.[3] Since for that problem the neutral axis of strain coincided with the geometrical center of the section, relatively simple expressions were developed relating M and ϕ. If, however, axial load in addition to the imposed moment is applied, such a condition will no longer exist.

The determination of M - ϕ curves including the effect of axial load has been developed by Timoshenko for the case of rectangular sections.* For the case of WF shapes discontinuities of the cross-section make direct computation troublesome. In the next section of this report a method suitable to handling such a problem is developed.

The purpose of this paper is to present a "point-by-point" method of computing M - ϕ curves similiar to that used earlier[3] including the influence of axial load and suitable for rolled sections. The method presented is not difficult to set-up and effectively illustrates the variables involved.

---

* Pages 51-54, Reference (2).

II. METHOD OF SOLUTION

When a member is loaded within the elastic range by combined bending and thrust, stress and strain diagrams similar to those shown in Fig. 4 result.

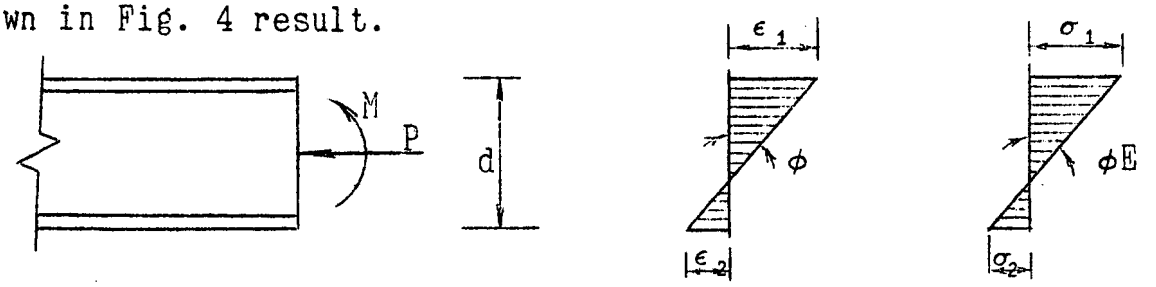

Strain Diagram Stress Diagram

Fig. 4

If $\Delta = \epsilon_1 - \epsilon_2$, using Timoshenko's notation, $\tan \phi = \Delta/d$. However, since the strains are small in comparison to the depth of the section, $\tan \phi = \phi$ or $\phi = \Delta / d$. But since $\Delta = \frac{\sigma_1 - \sigma_2}{E}$,

$$\phi = \frac{\sigma_1 - \sigma_2}{E d}$$

For members loaded beyond the elastic limit such as that shown in Fig. 5, a slightly different expression relating ϕ and σ is obtained.

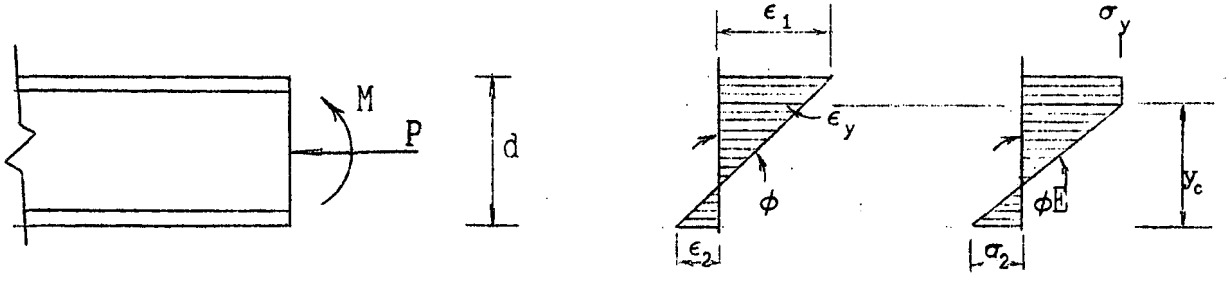

Strain Diagram Stress Diagram

Fig. 5

For these distributions of stress and strain

$$\phi = \frac{\epsilon_1 - \epsilon_2}{d} = \frac{\epsilon_y - \epsilon_2}{y_c}$$

or

$$\phi = \frac{\sigma_y - \sigma_2}{E y_c} \qquad \ldots\ldots\ldots\ldots\ldots\ldots (1)$$

Equation *(1)* is similar to that obtained for the elastic case except that y_c has replaced d, and σ_y replaced σ_1 . Therefore, it is possible to compute ϕ directly from a stress diagram providing that only that part of the section which remains elastic is considered.

From a stress diagram it is also possible to determine both the moment acting on the section and the applied thrust. These quantities are defined by the classic equations:*

$$P = \int_A \sigma \, dA \qquad \cdots\cdots\cdots\cdots\cdots\cdots\cdots\cdots (2)$$

$$M = \iint_{d\,A} \sigma \, dA \, y \, dy \qquad \cdots\cdots\cdots\cdots\cdots\cdots\cdots\cdots (3)$$

By using equations *(1)*, *(2)* and *(3)* it is then possible to determine M, P and ϕ for any given stress distribution.

When a member is subjected to both compressive forces and bending, yielding will first occur at the extreme fiber on the compression side of the specimen. As the load (that is, axial thrust and/or moment) is increased, yielding will penetrate through the flange on the compression side. After further yielding it will have penetrated to ¼ the depth of the section. Then ½ the depth, etc. Now consider what effect the tension side of the specimen has (for a given fixed value of yield penetration on the compression side) in determining the values of the external loads, P and M.

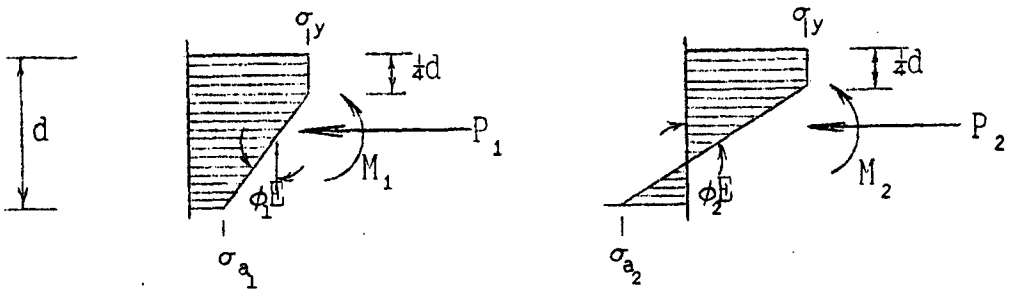

Fig. 6

---

* Pages 45-54, Reference (2).

Using Equations *(1)*, *(2)* and *(3)* each of the stress diagrams of Fig. 6 define distinct values of M, P and ϕ even though the net effect of each on the compression side has been to cause yielding to penetrate to a depth of $\frac{1}{4}$ the section. It is possible then by selecting various values of σ_a to determine M, P and ϕ* corresponding to each selection of σ_a, thereby making it possible to plot curves of P vs ϕ and M vs ϕ for any given value of yield penetration on the compression side. One such set of curves if shown in Fig. 7 for an 8WF31 section where yielding was assumed to have penetrated to a depth of $\frac{1}{4}$d from one side. These curves have been made non-dimensional by plotting P/P_y vs $\phi E/\sigma_y$ and M/M_y vs $\phi E/\sigma_y$. (Since M_y, E and σ_y would be constant for any particular section, this is, in fact, an M-ϕ curve.) For all points plotted the corresponding stress distribution diagrams have been shown.

This method of assuming a penetration of yielding on the compression side of the section and then determining curves of P vs ϕ and M vs ϕ can be carried out for any value of yield penetration. The ones investigated in this study are indicated by the stress distribution curves of Fig. 8.

a. Elastic Limit

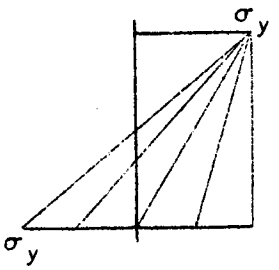

b. Yielding Penetrated Through Flange

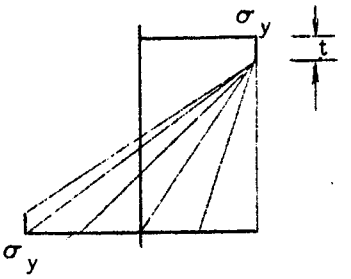

---

* Equation *(1)*, *(2)* and *(3)* are not in the most suitable form for determining M, P and ϕ for rolled sections due to the discontinuities resulting where the flanges and web join. Therefore, expanded equations in terms of the section dimensions have been given for WF shapes in Appendix A.

c. Yielding Penetrated to $\frac{1}{4}$ Depth of Section

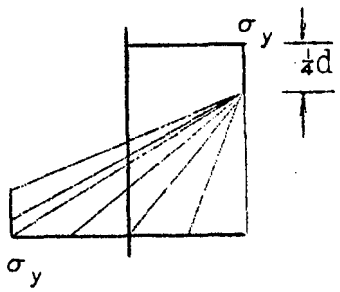

d. Yielding Penetrated to $\frac{1}{2}$ Depth of Section

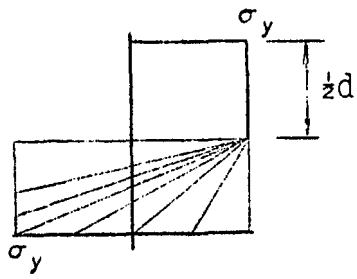

e. Yielding Penetrated to $\frac{3}{4}$ Depth of Section

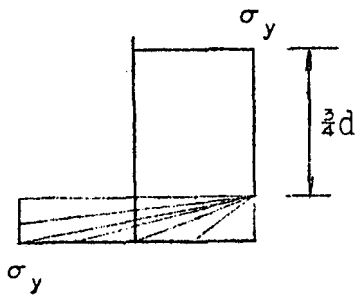

Fig. 8

Curves similar to Fig. 7 have been computed for each of these assumed values of yield penetration for the 8WF31 section. These are presented in Fig. 9. Since the straight line portion of each of these curves is that corresponding to an elastic stress condition on the tension (convex) side of the section, only the limiting cases where σ_a = yield point stress in compression and tension need be investigated to define that part of each curve. The limit of this range has been shown as a dash-dot line.

The general method of using these "auxiliary curves" (Fig. 9) is to select a value of P/P_y for which an $M-\phi$ curve is desired. For example $P = 0.2P_y$. With this value of P/P_y draw a horizontal line cutting the various auxiliary $P-\phi$ curves. At these points of intersection project verticals until they intersect the corresponding $M-\phi$ auxiliary diagrams. Connecting these points gives the desired $M-\phi$ curve including the effect

of an axial thrust of $0.2P_y$. (This process is indicated in Fig. 9 by dashed lines.) Fig. 10 is the desired curve with the auxiliary construction lines removed.

The curved portions of Fig. 9 have been plotted to a larger scale in Fig. 11 to facilitate greater accuracy in this graphical method. Here $M-\phi$ curves for several different values of P/P_y have been shown (dashed lines).

The influence of varying axial load for a greater range of P/P_y is illustrated in Fig. 12. Here $M-\phi$ curves have been plotted for various values of P/P_y ranging from 0 to 0.8. As indicated by the dashed line, only when P is relatively small will the tension flange be plastic. For that range where it remains elastic, only the straight line portion of each auxiliary curve need be considered to obtain the desired $M-\phi$ curve.

III. DISCUSSION

Since it is the integrated effect of curvature that determines the deflection of a structural member, and since design methods are indirectly based on deflection as the criterion of usefulness, it is important to consider the influence of axial thrust on the moment-curvature relation in the plastic range.*

The method for determining the M-ϕ curves presented in the previous section, while not the most direct solution to the problem, appears to be the easiest to use and best illustrates the variables involved. Possibly a more mathematical approach would be as follows: Each of equations *(4)*, *(5)* and *(6)*, corresponding to expanded equations *(1)*, *(2)* and *(3)*, contain 5 variables; M, P, ϕ, y_c, and (y_t or σ_a), where

M	=	Moment,
P	=	Concentric axial load,
ϕ	=	Curvature,
y_c	=	Distance from yield penetration in compression to extreme fiber in tension,
y_t	=	Depth of yield penetration in tension,
σ_a	=	Stress on tension side of section.

The formal procedure would be to eliminate the latter two of these unknowns thus obtaining an expression relating M and ϕ and including the variable P.** Instead of solving the problem in this manner, we have chosen a simpler point-by-point method. The procedure used however appears to give a clearer indication of the interrelationship between M, P and ϕ as stresses exceed the elastic limit.

---

* Deflection and rotation curves can be obtained by using Newmark's method for numerically integrating the M-ϕ curves defined in this report.

** This procedure is outlined in Appendix B.

Only one type of stress-strain curve has been considered in this paper. This one, which agrees comparatively well with mild structural steel coupon tests in the elastic and plastic ranges, is composed of two straight lines, one at a slope E up to the yield point and then the other horizontal. One method of extending the method developed herein to include the case of curved stress-strain diagrams would be to approximate the curved diagram with a series of straight lines[5]. Any degree of accuracy could then be achieved by increasing the number of straight-line segments; the resulting expression would be more complex.

Residual stresses would cause a deviation from the straight line portion of the $M-\phi$ curve at a smaller value of M than predicted by a theory that neglects their effect. The relative differences are greater for larger values of axial load. A partial solution to the problem of the effect of residual stresses on moment-curvature relations using experimentally measured residual stress distribution values has been obtained. In general, good agreement was noted between the curves resulting from that study and full scale column tests.* Solution of the $M-\phi$ relation including the effects of residual stresses will be presented in a future report.

More detailed studies of the problem of beam bending based of the various "theories of plasticity" have been presented by Aris Phillips in his various reports relating to ONR TASK ORDER 11.[6] These mathematical derivations frequently result in the solution of complex partial differential equations; however, the method gives an "exact theory of bending" provided all of the implied conditions of material behavior are fulfilled.

---

* See for example, Column Research Council Progress Report, Vol. IV, No. 2, April 1952, page 6.

IV. SUMMARY

A method has been developed for determining the influence of axial load on the moment-curvature relation in the plastic range. The method used employs a point-by-point procedure of determining "auxiliary curves"(Fig. 7 or Fig. 9) prior to obtaining the final M-ϕ relation (Fig. 10). However, once these "auxiliary curves" have been plotted for a particular section, the M-ϕ relation can be obtained conveniently for any desired value of axial load (Fig. 12).

V. ACKNOWLEDGEMENTS

The authors wish to express their appreciation to Mr. Don C. McCullough for the detailed numerical work of this report. The work is being carried out under the direction of the Lehigh Project Subcommittee of the Structural Steel Committee, Welding Research Council, at Fritz Engineering Laboratory of which Professor William J. Eney is Director.

VI. NOMENCLATURE

A	Area of cross-section
b	Flange width
d	Depth of section
E	Young's modulus of elasticity
M	Moment
M_y	Moment at which yield point is reached in flexure
P	Concentric axial load on a column
P_y	Axial load corresponding to yield point stress across entire section
S	Section modulus
t	Flange thickness
w	Web thickness
y_c	Distance from yield penetration in compression to extreme fiber in tension
y_t	Depth of yield penetration in tension
Δ	The difference in strains in the outermost fibers on the convex and the concave sides of a member
ϵ	Strain
ϵ_y	Strain corresponding to yield point stress
σ	Normal stress
σ_y	Lower yield point stress
ϕ	Curvature at a section (the reciprocal of the radius of curvature)

VII. REFERENCES

(1) Yang, C. H., "The Plastic Behavior of Steel Beams", Ph.D. Dissertation, Lehigh University, Jan. 1951.

(2) Timoshenko, S., "Theory of Elastic Stability", First Edition, McGraw-Hill Book Co., Inc., New York, 1936.

(3) Luxian, W. W., and Johnston, B. G., "Plastic Behavior of Wide Flange Beams", The Welding Journal Supplement A.W.S., vol. 27, No. 11, November 1948.

(4) Ketter, Robert L., Beedle, Lynn S., and Johnston, B. G., "Strength of Columns Under Combined Bending and Thrust", (scheduled for publication in the Welding Journal of the American Welding Society).

(5) Phillips, Aris, "Bending with Axial Force of Curved Bars in Plasticity", Technical Report No. 10, Division of Engineering Mechanics, Stanford University, June, 1951.

(6) Phillips, Aris, "Pure Bending with Axial Force in the Theory of Plastic Deformations", Technical Report No. 3, Division of Engineering Mechanics, Stanford University, Jan., 1949.

APPENDIX A

SUMMARY OF IMPORTANT EQUATIONS FOR DETERMINING M, P and ϕ

I. ELASTIC LIMIT CASE

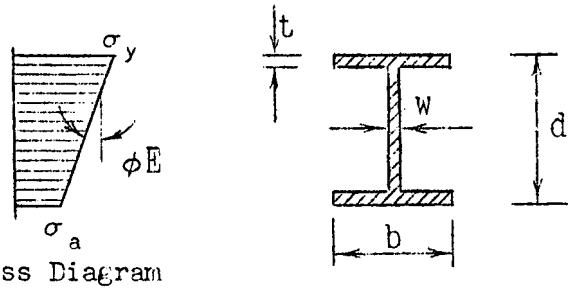

Stress Diagram

$$P = \frac{(\sigma_y+\sigma_a)}{2}\left[2bt + w(d-2t)\right]$$

$$M = (\sigma_y-\sigma_a)\left[\frac{bt}{6d}(3d^2-6dt+4t^2) + \frac{w}{12d}(d-2t)^3\right] \quad \cdots\cdots\cdots\cdots (4)$$

$$\phi = \frac{(\sigma_y-\sigma_a)}{Ed}$$

II. ONE FLANGE PLASTIC, THE OTHER ELASTIC

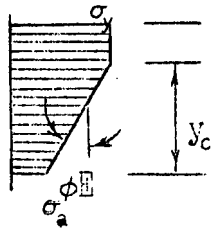

Limits:

$\sigma_a \geq -\sigma_y$

$y_c \leq (d-t)$

$$P = (\sigma_y+\sigma_a)\left[bt - wt\right] + (\sigma_y-\sigma_a)\left[\frac{bt^2}{2y_c} - \frac{wy_c}{2} - \frac{wt^2}{2y_c}\right] + wd\sigma_y$$

$$M = (\sigma_y+\sigma_a)\left[\frac{w}{12y_c}(y_c-t)^2(3d-2y_c-4t) + \frac{bt}{12y_c}(6y_cd-2y_ct-3dt+2t^2)\right] \cdots (5)$$

$$\phi = \frac{(\sigma_y+\sigma_a)}{E\,y_c}$$

III. BOTH FLANGES PLASTIC

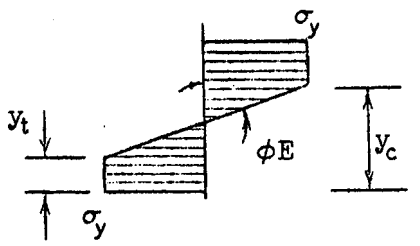

Limits:

$y_c < (d-t)$

$y_c > y_t > t$

$$P = w\sigma_y\left[d - y_t - y_c\right]$$

$$M = \sigma_y\left[bt(d-t) + w(y_t-t)(d-y_t-t) + \frac{w}{6}(y_c-y_t)(3d-2y_c-4y_t)\right] \quad \cdots\cdots (6)$$

$$\phi = \frac{2\sigma_y}{(y_c-y_t)E}$$

Note: The effect of the fillet has been neglected in these equations.

APPENDIX B

OUTLINE OF ALTERNATE METHOD OF M-ϕ SOLUTION

I. From equation *(5)*, page 14, (tension flange elastic)

(a) $\phi = \dfrac{(\sigma_y - \sigma_a)}{y_c E}$

(b) $M = (\sigma_y - \sigma_a)\dfrac{w}{12\, y_c}(y_c - t)^2 \left(\cdots\cdots \cdots \text{ etc.} \right)$

(c) $P = (\sigma_y + \sigma_a)\, bt - wt + \cdots\cdots \text{ etc.}$

1) Substitute the value of σ_a obtained from eq. (a) into eq. (b) and simplify. The resulting expression is of the form

$$M = E\phi\left[a_1 y_c^3 + b_1 y_c^2 + c_1 y_c + d_1\right] ,$$

where a_1, b_1, c_1 *and* d_1 are various geometrical constants of the section.

2) Make the same substitution in equation (c) and solve for y_c.

$$y_c = \sqrt{(a_2)^2 + \frac{b_2\sigma_y}{E\phi} + \frac{\sigma_y}{E\phi}\left[c_2 + \frac{d_2 P}{\sigma_y}\right] + e_2} \; - a_2$$

Here again a_2, b_2, c_2, d_2 *and* e_2 are geometrical constants.

3) Replace y_c in the moment equation with the expression determined in step 2). This will be the desired M-ϕ relation.

II. For the case where both flanges are plastic *(Eq. (6)*, page 15, the above outlined reasoning will result in the following equations:

1) $$M = \sigma_y\left[a_3 y_c^2 + b_3 y_c + \frac{c_3\sigma_y}{E\phi} y_c + \frac{d_3\sigma_y}{E\phi} + e_3\right]$$

2) $$y_c = \left[\frac{\sigma_y}{E\phi} + a_4 - \frac{P\, b_4}{\sigma_y}\right]$$

Therefore,

3) $$M = \sigma_y\left[\left(\frac{\sigma_y}{E\phi}\right)^2 a_5 + \frac{\sigma_y}{E\phi} b_5 + \left(\frac{P}{\sigma_y}\right)\left(c_5 + \frac{\sigma_y}{E\phi} d_5\right) + \left(\frac{P}{\sigma_y}\right)^2 e_5 + f_5\right]$$

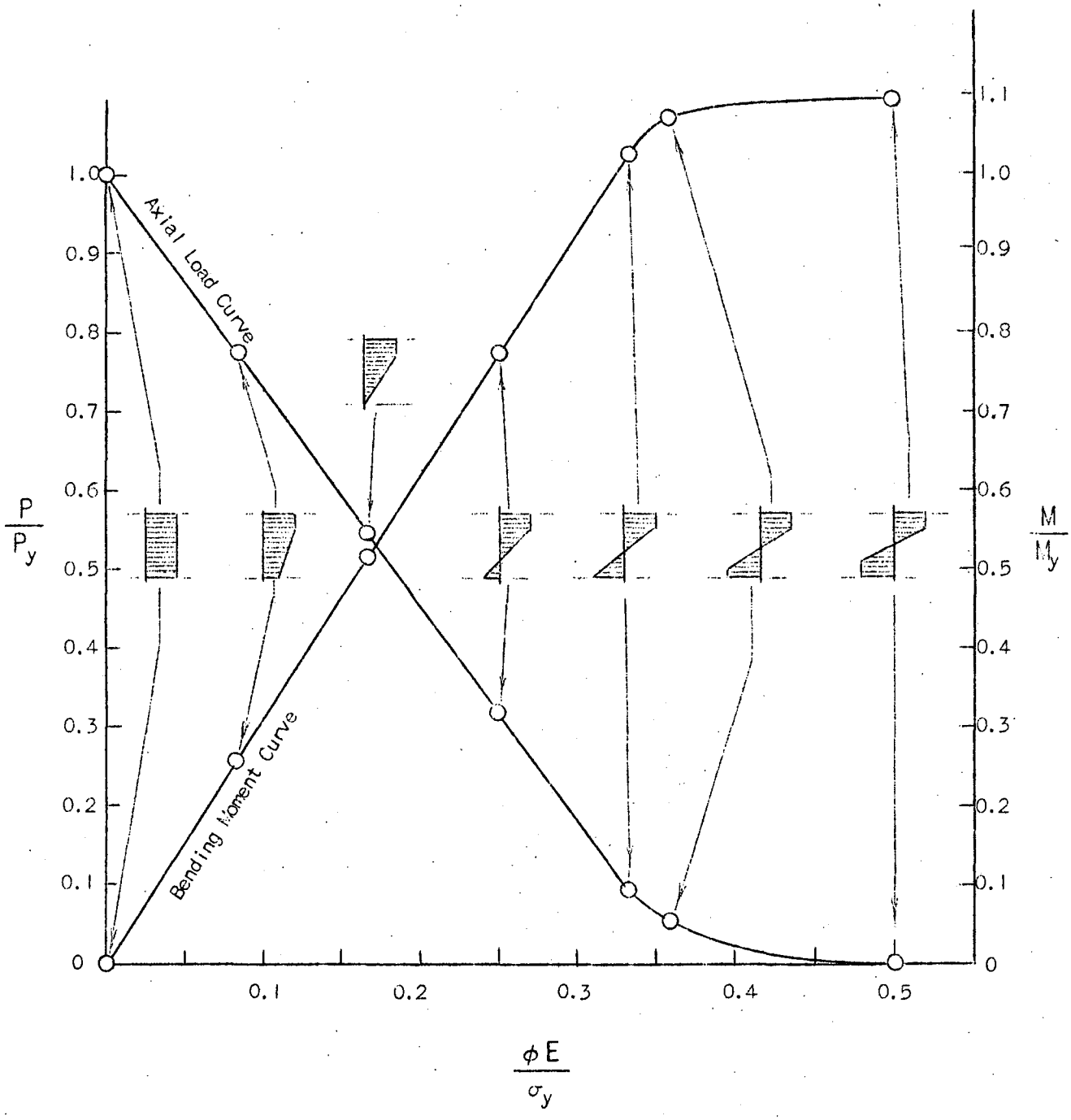
Axial Load Curve
Bending Moment Curve
P/Py
M/My
φE/σy
0
0.1
0.2
0.3
0.4
0.5
0.6
0.7
0.8
0.9
1.0
1.1

Fig. 7

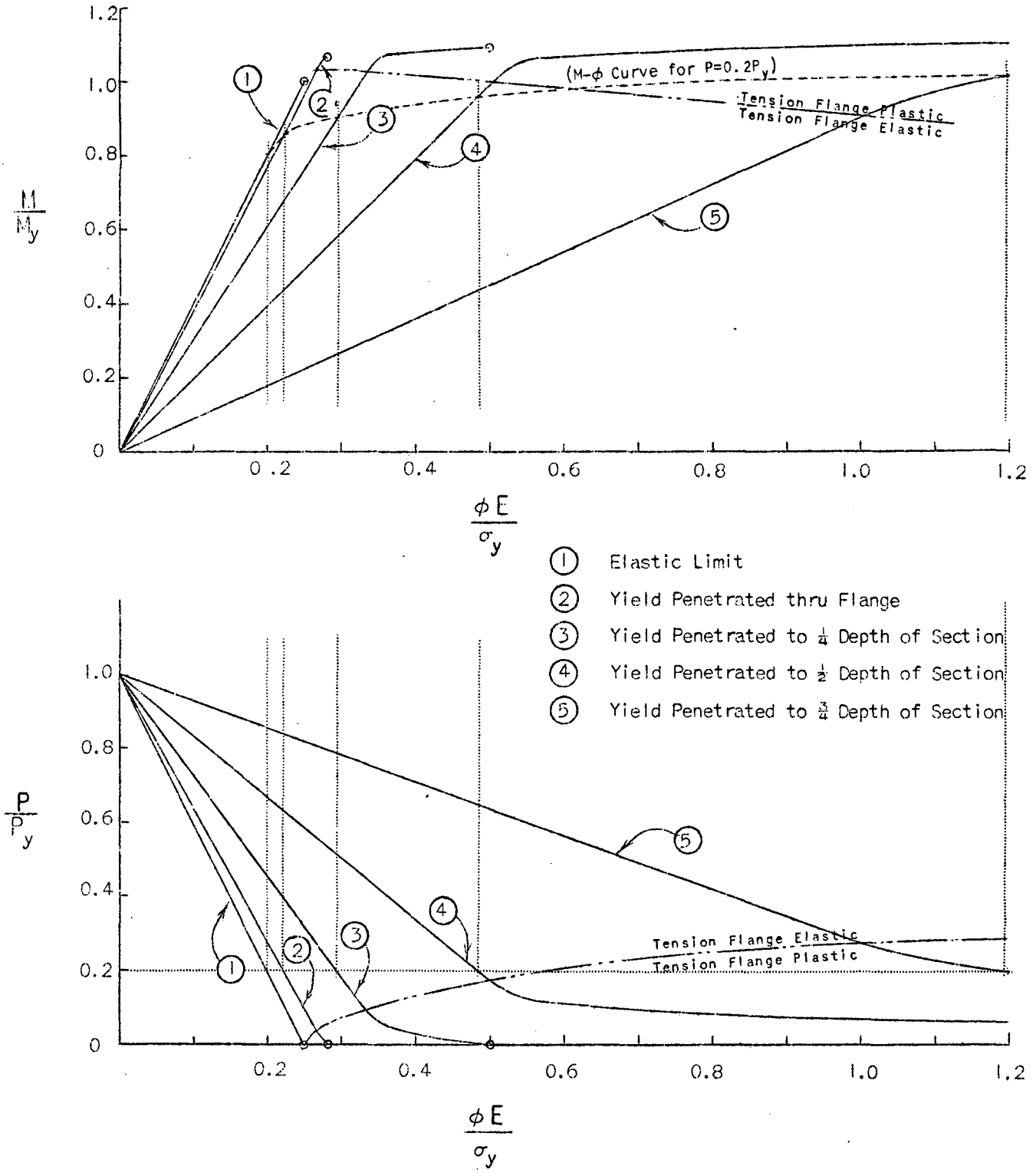
1.2
1.0
0.8
0.6
0.4
0.2
0
M/My
(M-φ Curve for P=0.2Py)
Tension Flange Plastic
Tension Flange Elastic
0.2
0.4
0.6
0.8
1.0
1.2
φE/σy
① Elastic Limit
② Yield Penetrated thru Flange
③ Yield Penetrated to ¼ Depth of Section
④ Yield Penetrated to ½ Depth of Section
⑤ Yield Penetrated to ¾ Depth of Section
P/Py
Tension Flange Elastic
Tension Flange Plastic
φE/σy

Fig. 9

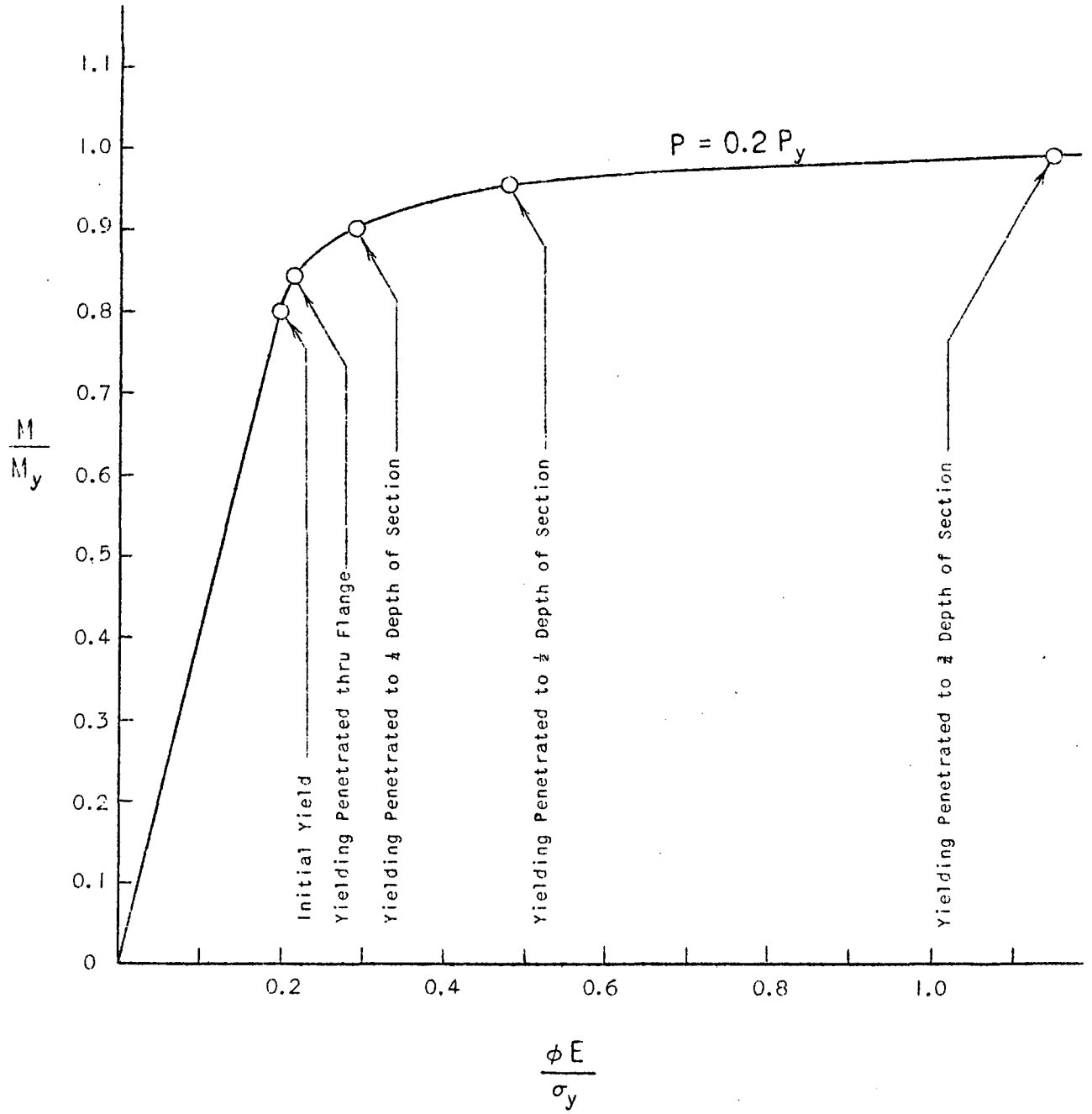
P = 0.2 Py
Initial Yield
Yielding Penetrated thru Flange
Yielding Penetrated to ¼ Depth of Section
Yielding Penetrated to ½ Depth of Section
Yielding Penetrated to ¾ Depth of Section
M / My
φE / σy
0
0.1
0.2
0.3
0.4
0.5
0.6
0.7
0.8
0.9
1.0
1.1
0.2
0.4
0.6
0.8
1.0

Fig. 10

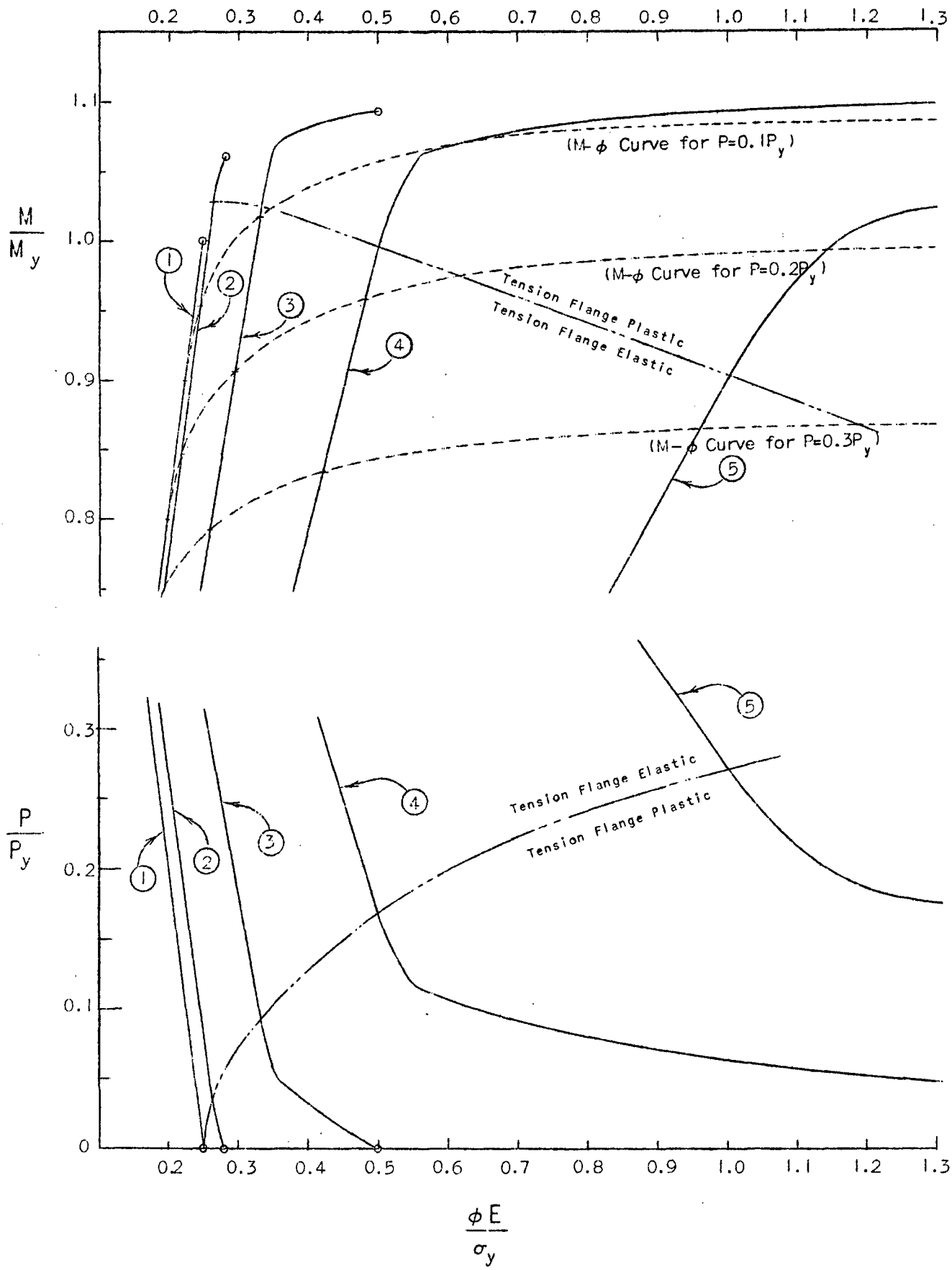
0.2 0.3 0.4 0.5 0.6 0.7 0.8 0.9 1.0 1.1 1.2 1.3
M / M_y
1.1
1.0
0.9
0.8
(M-φ Curve for P=0.1P_y)
(M-φ Curve for P=0.2P_y)
(M-φ Curve for P=0.3P_y)
Tension Flange Plastic
Tension Flange Elastic
1
2
3
4
5
P / P_y
0.3
0.2
0.1
0
Tension Flange Elastic
Tension Flange Plastic
φE / σ_y

Fig. 11

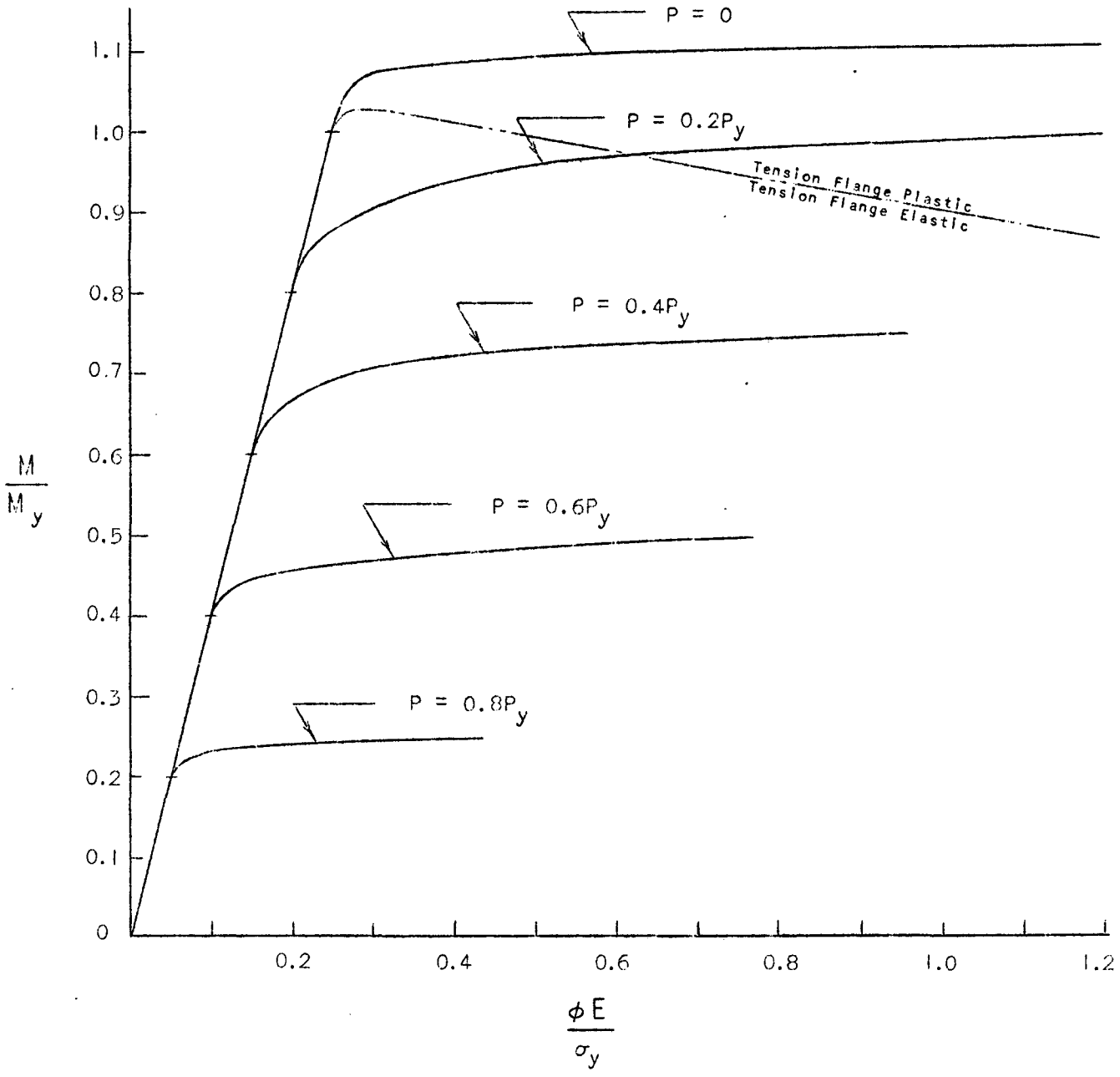
P = 0
P = 0.2Py
Tension Flange Plastic
Tension Flange Elastic
P = 0.4Py
P = 0.6Py
P = 0.8Py
M/My
φE/σy
0
0.1
0.2
0.3
0.4
0.5
0.6
0.7
0.8
0.9
1.0
1.1
0.2
0.4
0.6
0.8
1.0
1.2

Fig. 12

DIST. 9

February 18, 1952

DISTRIBUTION LIST
for
Technical and Final Reports Issued Under
Office of Naval Research Project NR-064-345. Contract N7onr-39303

Part I: Administrative, Reference and Liaison Activities of ONR

Chief of Naval Research
Department of the Navy
Washington 25, D. C.
Attn: Code 438 (1)

Director, Naval Research Lab.
Washington 25, D. C.
Attn: Tech. Info. Officer (9)
: Technical Library (1)
: Mechanics Division (2)

Commanding Officer
Office of Naval Research
Branch Office
495 Summer Street
Boston 10, Mass. (1)

Commanding Officer
Office of Naval Research
Branch Office
346 Broadway
New York 13, N. Y. (2)

Commanding Officer
Office of Naval Research
Branch Office
844 N. Rush Street
Chicago 11, Illinois (1)

Commanding Officer
Office of Naval Research
Branch Office
801 Donahue Street
San Francisco 24, Calif. (1)

Commanding Officer
Office of Naval Research
Branch Office
1030 Green Street
Pasadena, California (1)

Officer in Charge
Office of Naval Research
Branch Office, London
Navy No. 100
FPO, New York, N. Y. (5)

Library of Congress
Washington 25, D. C.
Attn: Navy Research Section (2)

Part II
Of Distribution List for Technical and Final Reports
Issued Under ONR Project NR -064-345

Department of Defense
Other Interested Government Activities
GENERAL

Research & Development Board
Department of Defense
Pentagon Building
Washington 25, D. C.
Attn: Library (Code 3D-1075) (1)

Armed Forces Special Weapons
Project
P. O. Box 2610
Washington, D. C.
Attn: Lt. Col. G.F. Blunda (1)

Joint Task Force 3
12 St. & Const. Ave. N.W.(Temp.U)
Washington 25, D. C.
Attn: Major B. D. Jones (1)

ARMY

Chief of Staff
Department of the Army
Research & Development Division
Washington 25, D. C.
Attn: Chief of Res. & Dev. (1)

Office of the Chief of Engineers
Assistant Chief for Works
Department of the Army
Bldg. T-7, Gravelly Point
Washington 25, D. C.
Attn: Structural Branch
(R. L. Bloor) (1)

Office of the Chief of Engineers
Asst. Chief for Military Construc.
Department of the Army
Bldg. T-7, Gravelly Point
Washington 25, D. C.
Attn: Structures Branch
(H. F. Carey) (1)
Protective Construction
Branch (I. O. Thorley) (1)

Office of the Chief of Engineers
Asst. Chief for Military Operations
Department of the Army
Bldg. T-7, Gravelly Point
Washington 25, D. C.
Attn: Structures Development
Branch (W. F. Woollard) (1)

Engineering Research & Development
Laboratory
Fort Belvoir, Virginia
Attn: Structures Branch (1)

The Commanding General
Sandia Base, P.O. Box 5100
Albuquerque, New Mexico
Attn: Col. Canterbury (1)

Operations Research Officer
Department of the Army
Ft. Lesley J. McNair
Washington 25, D. C.
Attn: Howard Brackney (1)

Office of Chief of Ordnance
Research & Development Service
Department of the Army
The Pentagon
Washington 25, D. C.
Attn: ORDTB (2)

Other Interested Government Activities

NAVY

Chief of Bureau of Ships
Navy Department
Washington 25, D. C.
Attn: Director of Research (2)
: Code 440 (1)
: Code 423 (1)
442 J.Vasta (2)
Director 350 (1)
David Taylor Model Basin
Washington 7, D. C.
Attn: Structural Mechanics
Division (2)

Director
Naval Engr. Experiment Station
Annapolis, Maryland (1)
Attn:
Director
Materials Laboratory
New York Naval Shipyard
Brooklyn 1, New York (1)

Chief of Bureau of Ordnance
Navy Department
Washington 25, D. C.
Attn: Ad-3, Technical Library (1)

Superintendent
Naval Gun Factory
Washington 25, D. C. (1)

Naval Ordnance Laboratory
White Oak, Maryland
RFD 1, Silver Spring, Maryland
Attn: Mechanics Division (2)

Naval Ordnance Test Station
Inyokern, California
Attn: Scientific Officer (1)

Naval Ordnance Test Station
Underwater Ordnance Division
Pasadena, California
Attn: Structures Division (1)

Chief of Bureau of Yards & Docks
Navy Department
Washington 25, D. C.
Attn: Code P-314 (1)
: Code C-313 (1)
P-300 (1)

Officer in Charge
Naval Civil Engr. Research and
Eval. Laboratory
Naval Station
Port Hueneme, California (2)

Superintendent, U.S. Naval
Post Graduate School
Annapolis, Maryland (1)

AIR FORCES

Commanding General
U. S. Air Forces
The Pentagon
Washington 25, D. C.
Attn: Research & Development
Division (1)

Office of Air Research
Wright-Patterson Air Force Base
Dayton, Ohio
Attn: Chief, Applied Mechanics
Group (1)

OTHER GOVERNMENT AGENCIES

U. S. Atomic Energy Commission
Division of Research
Washington, D. C. (1)

Director
National Bureau of Standards
Washington, D. C.
Attn: Dr. W. H. Ramberg (1)

U. S. Coast Guard
1300 E. Street, N. W.
Washington D. C.
Attn: Chief, Testing &
Development Division (1)

National Advisory Committee for
Aeronautics
Langley Field, Virginia
Attn: Mr. E. Lundquist (1)

U. S. Maritime Commission
Technical Bureau
Washington, D. C.
Attn: Mr. V. Russo (1)

Supplement A
To Distribution List for Technical and Final Reports
Issued Under ONR Project NR 064-345

Contractors and other Investigators Actively Engaged in Related Research

Professor Jesse Ormondroyd
University of Michigan
Ann Arbor, Michigan (1)

Dr. N. J. Hoff, Head
Department of Aeronautical
Engineering & Applied Mechanics
Polytechnic Inst. of Brooklyn
99 Livingston Street
Brooklyn 2, New York (1)

Dr. N. M. Newmark
Department of Civil Engineering
University of Illinois
Urbana, Illinois (1)

Dr. J. N. Goodier
School of Engineering
Stanford University
Stanford, California (1)

Dr. W. Osgood, Illinois
Institute of Technology
Technology Center
Chicago, Illinois (1)

Professor B. Fried
Washington State College
Pullman, Washington (1)

Dr. A. Phillips
School of Engineering
Stanford University
Stanford, California (1)

Dr. W. Prager
Graduate Division of Applied
Mathematics
Brown University
Providence, Rhode Island (1)

Professor L. S. Jacobsen
Stanford University
Stanford, California (1)

Dr. W. H. Hoppmann
Department of Applied Mechanics
Johns Hopkins University
Baltimore, Maryland (1)

Professor W. K. Krefeld
College of Engineering
Columbia University
New York, New York (1)

Professor R. M. Hermes
University of Santa Clara
Santa Clara, California (1)

Dr. R. P. Peterson
Director
Applied Physics Division
Sandia Laboratory
Albuquerque, New Mexico (2)

Dr. R. J. Hansen
Massachusetts Inst. of Technology
Cambridge 39, Mass. (1)

Professor Vito Salerno
Department of Aeronautical Engr.
and Applied Mechanics
Polytechnic Inst. of Brooklyn
85 Livingston St.
Brooklyn 2, N. Y. (1)

Library, Engineering Foundation
29 W. 39th Street
New York City, New York (1)

Members, Project Staff (5)

Project File (10)

Reserve copies for future distribution do not show on distribution list.

DATE DUE